Chemical and Functional Identification and Characterization of Novel Sulfated α-Conotoxins from the Cone Snail *Conus anemone*

Marion L. Loughnan,[†,||] Annette Nicke,[†,‡,§,||] Alun Jones,[†] David J. Adams,[‡] Paul F. Alewood,[†] and Richard J. Lewis*[,†,‡]

Institute for Molecular Biosciences, The University of Queensland, Brisbane, QLD 4072, Australia, and School of Biomedical Sciences, The University of Queensland, Brisbane, QLD 4072 Australia

Received August 18, 2003

An LC/MS analysis with diagnostic screening for the detection of peptides with posttranslational modifications revealed the presence of novel sulfated peptides within the α-conotoxin molecular mass range in *Conus anemone* crude venom. A functional assay of the extract showed activity at several neuronal nicotinic acetylcholine receptors (nAChRs). Three sulfated α-conotoxins (AnIA, AnIB, and AnIC) were identified by LC/MS and assay-directed fractionation and sequenced after purification. The most active of these, α-AnIB, was further characterized and used to investigate the influence of posttranslational modifications on affinity. Synthetic AnIB exhibited subnanomolar potency at the rat α3β2 nAChR (IC_{50} 0.3 nM) and was 200-fold less active on the rat α7 nAChR (IC_{50} 76 nM). The unsulfated peptide [Tyr[16]]AnIB showed a 2-fold and 10-fold decrease in activities at α3β2 (IC_{50} 0.6 nM) and α7 (IC_{50} 836 nM) nAChR, respectively. Likewise, removal of the C-terminal amide had a greater influence on potency at the α7 (IC_{50} 367 nM) than at the α3β2 nAChR (IC_{50} 0.5 nM). Stepwise removal of two N-terminal glycine residues revealed that these residues affect the binding kinetics of the peptide. Comparison with similar 4/7-α-conotoxin sequences suggests that residue 11 (alanine or glycine) and residue 14 (glutamine) constitute important determinants for α3β2 selectivity, whereas the C-terminal amidation and sulfation at tyrosine-16 favor α7 affinity.

Introduction

Conotoxins are small disulfide-rich peptides in the venom of predatory marine snails from the family *Conidae*. α-Conotoxins are competitive antagonists of nicotinic AChRs, pentameric ligand-gated cation channels which have been implicated in a variety of diseases and gain interest as drug targets for the treatment of several neurological disorders.[1,2] Eight α- and three β-subunits (α2−α7, α9, α10, β2−β4) of nAChRs have been cloned from neuronal mammalian cells.[1−3] These can assemble into a diversity of nAChR receptor subtypes with different pharmacological and functional properties. The identified α-conotoxins have been a useful source of subtype-selective ligands which will help to design optimized synthetic peptides for structure and function studies of the various nAChR subtypes.

There is a growing list of posttranslational modifications (PTMs) that contribute to the diversity of α-conopeptides. These include C-terminal amidation generally, proline hydroxylation and glutamic acid γ-carboxylation in GID,[4] and tyrosine sulfation identified in EpI, PnIA, and PnIB.[5,6] An analytical approach based on mass spectrometry (MS) is an important technique for identification and characterization of PTMs, including sulfation and phosphorylation in peptides and proteins.[6−9]

In this study we combined LC/MS techniques and a functional assay to identify three novel α-conotoxins, AnIA, AnIB, and AnIC, from *C. anemone*, a worm-hunting cone snail from southern Australian waters. The quantitatively and functionally dominant AnIB was selected for further characterization to determine the contributions of the sulfotyrosine and the C-terminus and the N-terminal glycine residues to binding to the rat α3β2 and α7 nAChRs. This is the first study to address the influence of these PTMs and the conserved N-terminal glycine on α-conotoxin activity at defined nAChRs and further extends the information on the structure−activity relationships among α-conotoxins.

Results and Discussion

Identification and Isolation of Peptides by Mass Spectometry. We used mass spectrometry to identify a number of sulfated and nonsulfated peptides with masses in the size range of α-conotoxins (1400−2200 Da) in the venom of *C. anemone*. LC/MS analysis of the crude venom and MS of individual fractions before and after reduction indicated the presence of several putative α-conotoxins containing two disulfide bonds. Experiments with diagnostic LC/MS scanning for sulfopeptides revealed that some of the venom components were likely to be sulfopeptides (Figure 1). MS and LC/MS of these components under standard mass spectrometric experimental conditions revealed two series of coeluting related ions corresponding to a mass difference of 80 Da, reflecting a partial loss of sulfur trioxide ($m = 80$ Da) from sulfopeptides or possibly a phosphate from phosphopeptides.

A "hi/lo" declustering experiment was performed in order to selectively detect sulfopeptides using positive ion detection mode. This involves the comparison of

* Coresponding author. Phone: +61 7 3346 2984. Fax: +61 7 3346 2101. E-mail: r.lewis@imb.uq.edu.au.
† Institute for Molecular Biosciences.
‡ School of Biomedical Sciences
§ Present address: Max Planck-Institute for Experimental Medicine, Hermann Rein-Str. 3, D-37075 Göttingen, Germany.
|| These two authors contributed equally to this work.

10.1021/jm031010o CCC: $27.50
Published on Web 01/29/2004

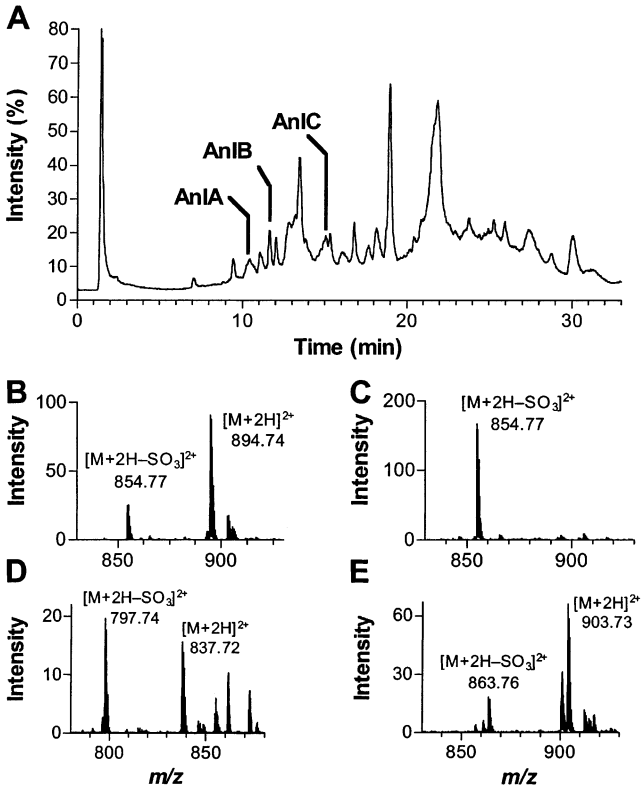

Figure 1. Multiexperiment approach using LC/ES-MS for the determination of sulfated peptides AnIA (1673.4 Da), AnIB (1787.4 Da), and AnIC (1805.4 Da) in the crude extract of *C. anemone*. (A) TIC of +TOF LC/ESMS over a range *m/z* 500−2200. Max 2.3e5 cps. Column: Zorbax 300SB C3 2.1 × 150 mm, 5 μm column, Gradient: 0 to 60%B in 60 min, A 0.1% formic acid, B 90% acetonitrile, aq, 0.09% formic acid, at 300 μL/min. The experiment shown was under low declustering energy conditions to minimize desulfation in MS. Location of the three selected components has been indicated. (B) ES mass spectrum of A revealing the presence of two sets of ions 80 Da apart, indicating sulfation or phosphorylation of tyrosine. The doubly charged ions 894.7 and 854.7 for AnIB M 1787.4 and 1707.4 Da are shown (11.5−11.7 min, max. 164.3 counts). The experiment shown was under low declustering energy conditions to minimize desulfation in MS. (C) ES mass spectrum of A revealing the extensive loss of the doubly charged ion at 894.7, corresponding to the loss of an 80 Da sulfate or phosphate group from a tyrosine residue. The doubly charged ion at 854.7 for AnIB M-SO_4 1707.4 Da is shown. The experiment shown was under high declustering energy conditions to enhance desulfation in MS. (D) ES mass spectrum of A revealing the presence of two sets of ions 80 Da apart, indicating sulfation or phosphorylation of tyrosine. The doubly charged ions 837.7 and 797.7 for AnIA M 1673.4 and 1593.4 Da are shown (10.3−10.5 min, max. 36.9 counts). The experiment shown was under low declustering energy conditions to minimize desulfation in MS. (E) ES mass spectrum of A revealing the presence of two sets of ions 80 Da apart, indicating sulfation or phosphorylation of tyrosine. The doubly charged ions 903.7 and 863.8 for AnIC M 1805.4 and 1725.5 Da are shown (14.9−15.1 min, max. 57.8 counts). The experiment shown was under low declustering energy conditions to minimize desulfation in MS.

mass spectra from high and low declustering potential experiments, specifically for the mass difference of 80 Da, corresponding to the loss of SO_3. A high declustering potential is capable of breaking the SO_3 attachment to the peptide under positive ion conditions whereas a low declustering potential can preserve the otherwise labile SO_3 attachment. An additional experiment using negative ion detection mode to utilize the ability of the SO_3 group to hold a negative charge and thus preserve its attachment to the peptide was performed to confirm and complement the results of the "hi/lo" declustering energy experiment for identification of the presence of a sulfated residue (data not shown). A final experiment (data not shown) involved the acquisition of product ion spectra in the positive ion mode to produce amino acid sequence data that failed to show evidence of a phosphorylated tyrosine, which would be indicated by the presence of the immonium ion at *m/z* 216.04.[7] The combination high and low energy experiment resulted in two mass spectra which clearly showed extensive loss of the 80 Da SO_3 group at higher collision energy conditions, and reduced loss at lower collision energy conditions for those components (Figure 1). The sulfur trioxide moiety of a sulfopeptide is relatively stable in negative ion mode LC/MS conditions compared to its lability in positive ion mode LC/MS,[7] and the mass spectra obtained in negative ion mode showed the mass values of the intact sulfopeptides as expected (data not shown). The different stability of the two modification groups in negative ion mode and positive ion mode LC/MS distinguishes phosphorylation and sulfation although both moieties have a nominal mass of 80 Da.[7] Thus although the observed loss of 80 Da from the precursor could also be attributable to presence of a phosphopeptide, the lability under high energy positive ion mode LC/MS conditions, and the stability under both low energy positive ion mode LC/MS and negative ion mode LC/MS conditions, are characteristic of sulfopeptides. Taken together, these results support the conclusion that the conopeptides identifed are sulfated rather than phosphorylated, just as previously determined for EpI.[5]

Three peptides were isolated by MS-directed fractionation, assessed further by MS after purification, and sequenced by automated Edman chemistry. The variation in stability under different MS conditions together with the mass difference calculated from the primary sequences determined by Edman degradation (Table 1) reaffirmed that the peptides have a modification with either sulfation or less likely phosphorylation. MS after reduction confirmed that the native peptides contained two disulfide bonds, and their activity at nAChRs (see below) indicated that the peptides were new sulfated 4/7 α-conotoxins that we named An1A, AnIB, and AnIC (1673, 1787, and 1805 Da, respectively) (Table 1). An1A is a variant of AnIB with two deletions of glycine in positions one and two (des-G^1,G^2-AnIB). It was present in relatively low amounts and was not distinguished in fractionated venom in the functional assay.

The *C. anemone* peptides identified here extend the list of sulfopeptides that includes EpI, PnIA, and PnIB.[5,6] Other α-conotoxins such as AuIA and AuIC are reported to be unsulfated although they have a tyrosine residue in an equivalent position as found in the sulfated α-conotoxins (Table 2[10]). The new sequences described here may help to define consensus sequence motifs for sulfation in conotoxins. Presently, any function of tyrosine sulfation for α-conotoxins is not clear. Sulfation may contribute to the biophysical properties of the peptide and help stabilize or solubilize it. For example, a reduced solubility of [Tyr^{15}]EpI was previ-

Table 1. *C. anemone* α-Conotoxins Detected by LC/MS, Showing Mass Values, Including Sulfation, and Sequences (named in order of increasing hydrophobicity)

name	sequence[a]	mass (Da)[b] predicted	mass (Da)[b] observed (M, M − SO_3)
	Native Peptides		
AnIA	**CC**SH**P**A**C**AANNQDY**C***	1673.6	1673.4, 1593.4
AnIB	GG**CC**SH**P**A**C**AANNQDY**C***	1787.6	1787.4, 1707.4
AnIC	GG**CC**SH**P**A**C**FASNPDY**C***	1805.6	1805.4, 1725.5
	Synthetic Peptides		
AnIB	GG**CC**SH**P**A**C**AANNQDY**C***	1787.6	1787.5, 1707.5
[Y^{16}]AnIB	GG**CC**SH**P**A**C**AANNQDY**C***	1707.6	1707.5
AnIB-OH	GG**CC**SH**P**A**C**AANNQDY**C#**	1788.6	1788.5, 1708.5
[Y^{16}]AnIB-OH	GG**CC**SH**P**A**C**AANNQDY**C#**	1708.6	1708.5
Des-G^1-AnIB	G**CC**SH**P**A**C**AANNQDY**C***	1730.6	1730.8, 1650.8
AnIA	**CC**SH**P**A**C**AANNQDY**C***	1673.6	1673.4, 1593.4
G-AnIB	GGG**CC**SH**P**A**C**AANNQDY**C***	1844.6	1844.7, 1764.7

[a] Abbreviations: * denotes amidated C-terminus, # denotes carboxyl C-terminus, and Y denotes sulfotyrosine. [b] Predicted mass and observed mass (monoisotopic) for components with disulfide bonds intact are indicated.

Table 2. Comparison of Known α-Conotoxins from α4/7, α4/6, and α4/3 Families and Their nAChR Subtype Selectivity[a]

name	sequence[b]	target	reference
ImI	G**CC**SD**P**R**C**AWR- - - -**C***	α7	21
ImIIA	Y**CC**HRG**PC**MVW- - - -**C***		22
ImII	A**CC**SDRR**C**RWR- - - -**C***	α7	23
AuIB	G**CC**SY**P**P**C**FATNPD-**C***	α3/β4	10
AuIA	G**CC**SY**P**P**C**FATNSDY**C***	less active	10
AuIC	G**CC**SY**P**P**C**FATNSGY**C***	less active	10
MII	G**CC**SN**P**V**C**HLEHSNL**C***	α3/β2	24
EpI	G**CC**SD**P**R**C**NMNNPDY**C***	α3/β2, α3/β4; α7[c]	5, 11[c]
PnIA	G**CC**SL**P**P**C**AANNPDY**C***	α3/β2 > α7	6, 13
[A10L]PnIA	G**CC**SL**P**P**C**ALNNPDY**C***	α7 > α3/β2	14, 15, 16
PnIB	G**CC**SL**P**P**C**ALSNPD*Y***C***	α7 > α3/β2	6, 13
GIC	G**CC**SH**P**A**C**AGNNQHI**C***	α3/β2	25
GID	IRDγ**CC**SN**P**A**C**RVNNOHV**C#**	α3/β2, α7 > α4/β2	4
EI	RDO**CC**YH**P**T**C**NMSNPQI**C***	muscular nAChR	26
PIA	RDP**CC**SN**P**V**C**TVHNPQI**C***	α6β2β3	27
Vc1.1	G**CC**SD**P**R**C**NYDHPEI**C***	α3α7β4/α3α5β4	28
AnIB	GG**CC**SH**P**A**C**AANNQD*Y***C***	α3/β2, α7	this study

[a] Most α-conotoxins were tested at rat neuronal nAChR subunits expressed in *Xenopus* oocytes, except for GIC which was tested at human subunits expressed in *Xenopus* oocytes, and Vc1.1 which was tested in bovine chromaffin cells. [b] Asterisks indicate an amidated C-terminus. The symbol γ denotes γ-carboxyglutamic acid. The letters O and Y denote hydroxyproline and sulfotyrosine, respectively. The letter Y denotes sulfotyrosine identified after original sequence was published. Hyphens indicate gaps in the sequence alignment. [c] Selectivity of EpI varies depending on the functional assay systems investigated.[11]

ously observed (Loughnan and Gehrmann, unpublished observations). To test for a possible function in binding to its target nAChRs, we compared sulfated and non-sulfated AnIB analogues at two rat nAChR subtype combinations as described below.

Identification and Isolation of α-Conotoxins by a Functional Assay. In a parallel approach, we screened *C. anemone* crude venom and fractions for their ability to inhibit agonist-evoked currents of different combinations of rat neuronal nAChR subunits (α3β2, α3β4, α4β2, α4β4, and α7) heterologously expressed in *Xenopus* oocytes. Crude venom extract from *C. anemone* (50 μg protein/mL, total protein estimated from BCA assay (Pierce) caused a 100% and 98% block of the α3β2 and α7 nAChR subtypes, respectively, and 53−56% block of the α3β4 and α4β2 subtypes. No significant activity was detected at the α4β4 subtype. The crude venom was also tested in preliminary screening at the rat muscle nAChR (α1β1γδ) subtype heterologously expressed in *Xenopus* oocytes and caused no inhibition of ACh-evoked currents at doses that caused complete inhibition at the α3β2 nAChR (data not shown). Assay of fractionated crude venom at the α3β2 nAChR indicated the presence of active components in two adjacent α-conotoxin enriched SE fractions. Further assay-directed fractionation at the α3β2 nAChR was used to isolate new α-conotoxins. Predominant activity was found in a single 1 min RP-HPLC fraction eluting at 23 min that contained the 1787 Da sulfated component AnIB.

Chemical Synthesis of the Peptide AnIB and Several Analogues. The most significant of the peptides in terms of quantity and activity was AnIB. It was synthesized to confirm the identification of the sequence and the mass spectrometry interpretation and to determine the potency and subtype selectivity. Two variants of AnIB, without tyrosine sulfation or without C-terminal amidation, were also synthesized and assayed in order to investigate a possible influence of posttranslational modifications on the toxin activity. AnIB differs from most other α-conotoxins by having an additional N-terminal glycine residue. To investigate the role played by this unusual N-terminal tail, further analogues were synthesized in which one or two of the N-terminal glycine residues were removed or a third glycine residue was added to the sequence The seven synthetic peptides are shown in Table 1. Chromatography coelution and activity assay tests confirmed that the sulfated amidated peptide was identical to the native peptide (data not shown). The synthetic ana-

Table 3. IC_{50} Values (nM), 95% Confidence Intervals (CI), and Hill Slopes (n_H) for Inhibition of Agonist-Evoked Current by AnIB or AnIB Variants at Rat α3β2 and α7 nAChR Subtypes Expressed in *Xenopus* Oocytes

nAChR subtype	α3β2			α7		
α-conotoxin	IC_{50} mean	IC_{50} 95% CI	Hill slope	IC_{50} mean	IC_{50} 95% CI	Hill slope
AnIB	0.28	0.24−0.32	−1.06	76	68−85	−1.22
[Tyr^{16}]AnIB	0.64	0.56−0.73	−0.82	836	785−890	−1.30
AnIB-OH	0.54	0.49−0.60	−1.07	367	282−478	−1.26
Des-Gly^1-AnIB	0.17	0.13−0.22	−0.67	n.d.	n.d.	n.d.
AnIA	5.84	4.59−7.43	−0.85	n.d.	n.d.	n.d.
Gly-AnIB	0.20	0.17−0.24	−1.16	n.d.	n.d.	n.d.

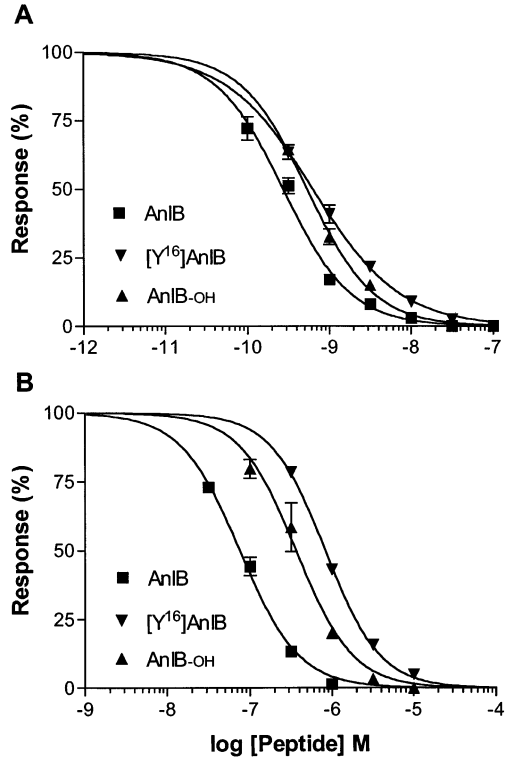

Figure 2. Activity of synthetic AnIB and AnIB PTM variants (unsulfated or C-terminally carboxylated) at (A) α3β2 and (B) α7 rat nAChRs expressed in *Xenopus* oocytes. Oocytes were voltage-clamped, and current responses were induced by 1 s application of 100 μM acetycholine (α3β2) or 100 μM nicotine (α7). Amidated (filled square), nonsulfated (filled downward triangle), and nonamidated (filled upward triangle) AnIB or AnIB variants were added 3−15 min prior to application of agonist. Responses are expressed as percentage of control current responses (without peptide). Error bars are SEM and $n = 3-4$ for each data point. IC_{50} values and Hill slope coefficients are summarized in Table 3.

logues with sulfation and C-terminus variations were distinctive in that oxidation of those peptides resulted in two substantial and closely eluting isoforms, whereas oxidation of AnIB resulted in one dominant isoform. Oxidation of the analogues des-G^1-AnIB, and AnIA (equivalent to des-G^1, G^2-AnIB) generated one major isoform and a minor poorly resolved isoform, but the G-AnIB analogue resulted in two major isoforms that were separable by HPLC (data not shown).

Functional Characterization of Synthetic AnIB and Analogues. Subtype Selectivity of sAnIB and Effect of PTMs. The potency and subtype selectivity of synthetic AnIB, the major characterized peptide, was determined at rat neuronal α3β2, α3β4, and α4β2 combinations, the α7 subtype, and the muscle α1β2γδ combination. AnIB showed subnanomolar activity at the α3β2 combination, with an IC_{50} value of 0.3 nM (Figure 2A, Table 3). The activity at the α7 nAChR was about 200-fold less (IC_{50} 76 nM; Figure 2B, Table 3). In contrast, 1 μM AnIB caused about 50% inhibition on the α3β4 and α4β2 combinations. On these two combinations, however, exact values were difficult to determine since the agonist solution was not supplemented with toxin (in order to reduce peptide usage), resulting in dissociation of the toxins from these receptors during the 1−2 s agonist application. AnIB (100 μM) exhibited no activity at the rat muscle nAChR (data not shown). The potency at the α3β2 receptor and selectivity profile of AnIB is very similar to that of α-conotoxin MII, the most potent and α3β2-selective α-conotoxin identified to date. The sequence, however, differs markedly from that of MII and places AnIB in a subclass of α4/7-conotoxins with a common AX_1NNX_2 (X_2 = O/P or Q) motif in the second loop (Table 4).

Table 4. Five α-Conotoxins Possessing a Common AXNNX Motif in the Second Loop and Their IC_{50} Values and α7/α3β2 Selectivities[a]

α-conotoxin	α3β2 (nM)	α7 (nM)	α3β2/α7 ratio	consensus sequence	reference
GIC	1.1	n.d.	−	CA**G**NN**Q**	25
AnIB	0.3	76	0.004	CA**A**NN**Q**	this study
PnIA	9.6	252	0.04	CA**A**NNP	15
[R12A]GID	10	48	0.2	CA**V**NNO	4
[A10L]PnIA	99	12.6	7.9	CA**L**NNP	15
MII	0.5	∼200	0.0025	CH**L**EHS	24

[a] In contrast, MII has a significantly different sequence motif and pharmacology to these α-conotoxins, suggesting that it has a different binding mode and targets a different microdomain at the ACh binding site.

The contributions of the PTMs to activity and subtype-selectivity of AnIB were identified by determining the activities of the nonamidated and nonsulfated analogues at the rat α3β2 and α7 nAChRs. Neither tyrosine-sulfation nor -amidation of the C-terminus facilitated binding to the α3β2 interface, since the nonsulfated and nonamidated analogues had only slightly reduced potency at this subtype (EC_{50} values of 0.6 nM and 0.5 nM, respectively) than the wild-type AnIB (Table 3). In contrast, the nonsulfated and nonamidated analogues had 10-fold and 5-fold reduced activity at the α7 nAChR (Table 3), indicating that both modifications differentially affect the binding to distinct nAChR subtypes and thus are able to contribute to subtype selectivity. In agreement with this, a 4-fold difference in the activities of sulfated and nonsulfated α-conotoxins at oocyte-expressed α7 nAChRs has also been observed for α-conotoxin EpI.[11]

The significance of the effect of sulfation of α-AnIB on activity at the α7 nAChR is not readily apparent. The effects of the PTMs of some α-conotoxins on structure and function are a matter of speculation and presumably relate to improved targeting of α-conotoxins

to the nAChR subtypes found in the prey species they hunt. More generally, protein and peptide sulfation is thought to have a number of roles ranging from altered biological activity as observed here to modulation of intracellular protein transport and altered susceptibility to proteolytic processing.[7,12] Limited if any comparisons have been done with the sulfopeptides EpI, PnIA, and PnIB and their unsulfated analogues[5,6] (Table 2). The peptides PnIA and PnIB were first reported as their primary unmodified sequences.[13] There is some confusion as to whether subtype specificities reported for PnIA and PnIB refer to the sulfated forms or unsulfated variants of these peptides. The subtype specificity reported for [A10L]PnIA[14−16] actually refers to the unsulfated form.

Influence of the N-Terminal Sequence on the Dissociation Rate. Inhibition of the rat α7 nAChR by AnIB and its analogues was rapidly reversible, with 100% recovery of responses seen after 3 min (data not shown). Recovery of the α3β2 subtype from AnIB block was significantly slower, requiring approximately 12 min. AnIB differs from most other 4/7 α-conotoxins in having a second N-terminal glycine residue. An N-terminal extension comprising three additional amino acid residues has previously been described for α-conotoxin GID and has been shown to affect the off-rate but not the potency of GID on the α3β2 and α7 nAChRs.[4] To investigate whether N-terminal extensions could provide a general way to affect binding kinetics without changing the potency, we compared the α3β2 affinity and off-rates of a series of AnIB analogues containing 0−3 glycine residues before the first conserved cysteine residue. Deletion of only one glycine residue from AnIB did not significantly influence potency of the peptide (IC_{50}: 0.28 and 0.17 nM for AnIB and des-G^1-AnIB, respectively; Figure 3A, Table 3) but increased the dissociation constant from 0.28 min^{-1} to 0.51 min^{-1}. Removal of the second glycine residue caused an even further increase of the dissociation constant to an estimated value of 2 min^{-1} and reduced the potency about 20-fold (IC_{50} of 5.8 nM) compared to AnIB (Figure 3A, Table 3). This was unexpected since in α-GID, deletion of the first four amino acids (which include the γ-carboxyglutamate in the equivalent position to Gly2 in AnIB and the conserved Gly1 in other conotoxins) did not cause a notable change in the IC_{50} values at the α3β2 and α7 nAChRs.[4] The clear effect on AnIB activity caused by the removal of this residue suggests that AnIB and GID have different binding modes at the α3β2 nAChR. However, the sequence similarity and the selectivity profile (Table 3) strongly indicate that both toxins have similar interactions with amino acid residues at the acetylcholine binding site. Therefore, a more plausible explanation is that the apparently absent effect on the IC_{50} value for GID is actually masked by a faster on-rate of the much shorter des-(1−4)-GID. Thus a slow on-rate and a slow off-rate in GID result in the same IC_{50} value as a fast on-rate and a fast off-rate in des-(1−4)-GID. AnIB, on the other hand, has a relatively fast on-rate, so that the increase in the off-rate caused by removal of the second glycine results in a shift of the IC_{50} value (Figure 3B).

Addition of one glycine residue to the N-terminus of AnIB did not markedly alter either the dissociation

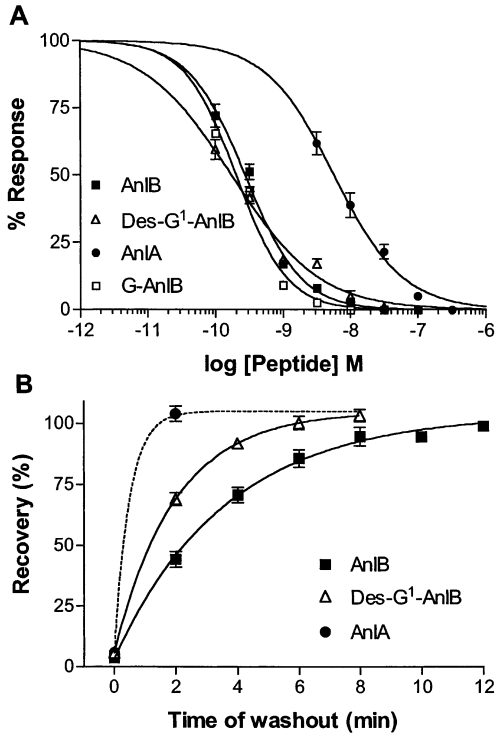

Figure 3. Concentration−response curves and off-kinetics of synthetic AnIB (filled square) and N-terminal glycine variants des-G^1−AnIB (open diamond), AnIA (equivalent to des-G^1,G^2−AnIB), (filled circle), and G-AnIB (open square), (concentration response curve only), at oocyte-expressed rat α3β2 nAChRs. Error bars are SEM and $n = 3-4$ for each data point. (A) Responses to 1 s application of ACh. (B) Recovery from maximal block after toxin was washed out. The line for AnIA (des-G^1,G^2−AnIB) is dashed to indicate an approximation.

constant (k_{off} 0.34 min^{-1}) or the activity (IC_{50} 0.2 nM) of the peptide at the α3β2 receptor. This indicates that specific interactions of the N-terminus are required to stabilize the receptor−peptide complex and that the N-terminal tail in GID, although unstructured and flexible in solution, makes specific interactions and attains a fixed conformation once it has reached its binding site. Taken together, these findings provide additional details on the binding mode of α-conotoxins that might aid the design of slowly dissociating α-conotoxins that could be useful in the establishment of radioligand binding assays.

Significance

The nAChRs are important targets for drug development.[17] However, selective ligands are needed to elucidate the physiological function and pharmacology of the numerous nAChR subtypes present in different neuronal tissues. Neuronal-specific α-conotoxins are highly selective nAChR antagonists. Structure−activity relationship studies of several native α-conotoxins with high selectivity for the α7-, α3β2-, and α3β4-subtypes of the neuronal nAChRs have already been developed.[18] These provide a foundation for the rational development of ligands with tailored selectivity. A goal of the present work has been to test strategies for the identification of further novel subtype selective α-conopeptides that might help define determinants for nAChR subtype selectivity. Three novel α-conotoxin sequences were identified using MS and peptide chemistry methodology

together with functional assays. The sequence and activity of AnIB, the predominant toxin identified, extended previously defined structure−activity relationships for α3β2 and α7 subtype selectivity for this class of α-conotoxin. Two posttranslational modifications, sulfated tyrosine and C-terminal amidation, were found to influence the binding of AnIB to mammalian α7 but not α3β2 subtypes. Thus the removal of the *O*-tyrosine sulfation improves selectivity for α3β2 over α7 nAChRs, which may have implications for the design of subtype specific variants of α-conotoxins. The addition of a third N-terminal glycine residue had little influence on potency, whereas sequential removal of one or two glycine residues had an important influence on off-rate kinetics at the α3β2 subtype. This effect of the N-terminal tail of AnIB may be useful in the design of α-conotoxin variants with slower off-rates that facilitate the development of subtype-specific radioligand binding assays.

Experimental Section

Peptide Characterization. Crude Venom Extraction. Thirty-five specimens of *C. anemone* were collected from the Mornington Peninsula, Victoria, Australia. A crude extract was prepared from venom duct material using 30% acetonitrile/water acidified with 0.1% TFA, and the material was centrifuged. Soluble material was lyophilized and stored at −20 °C prior to use.

Crude Venom Refinement. A portion of the crude venom extract (10 mg) was fractionated by size-exclusion chromatography (Superdex Peptide, HR 10/30, Pharmacia) in order to prepare a refined venom sample containing small peptides. Chromatography conditions were elution with 30% acetonitrile/0.048% TFA at a flow rate of 0.5 mL/min, with detection at 214 nm. Fractions were taken according to a predetermined calibration of the column to provide pools of material in defined size ranges. One of these was an α-conotoxin-inclusive small peptide fraction of approximately 1000−2500 Da.

LC/MS Analyses of Native Peptides from *C. anemone* Venom. The materials analyzed were a crude venom sample and a refined sample generated by size-exclusion chromatography to obtain a fraction enriched in components in the size range ∼1000−2500 Da, prepared as described above. LC/MS analysis was undertaken using a PESciex API QSTAR Pulsar instrument over a range *m*/*z* 500−2200. LC conditions were: Zorbax C3 2.1 × 150 mm, 5 μm column, eluted with 0 to 60%B in 60 min, A 0.1% formic acid, B 90% acetonitrile, aqueous 0.09% formic acid, at 300 μL/min.

Duplicate LC/MS analyses were run with first a positive mode "hi/lo" declustering LC/MS experiment and second a negative mode LC/MS experiment. These experiments were designed to assist in the identification of sulfopeptides. The positive ion detection mode "hi/lo" declustering experiment was undertaken to selectively detect sulfopeptides. Mass spectra from high and low declustering potential experiments were compared specifically for the mass difference of 80 Da corresponding to the loss of an SO_3 moiety under these conditions. The declustering potential is altered by adjusting the declustering (DP) and focusing (FP) voltage potentials. The SO_3 attachment to the peptide is labile under positive ion conditions with a high declustering potential produced by increasing the voltage potentials. Lowering the voltage produces a low declustering potential to preserve the labile SO_3 attachment. The declustering takes place in the Q0 region of the mass spectrometer and is also described as Q0 collision-induced dissociation (Q0 CID), as opposed to the conventional CID taking place in the collision cell after the first mass to charge resolving quadrupole. An additional experiment using negative ion detection mode was undertaken to complement the "hi/lo" declustering experiment for identification of the presence of a sulfotyrosine residue. A further experiment (data not shown) involving the acquisition of product ion spectra in the positive ion mode was used to produce amino acid sequence data and to search for phosphorylated tyrosine by the presence of its immonium ion at *m*/*z* 216.04.[7]

Isolation and Purification of Native Peptides. A second portion of the crude venom extract was fractionated using semipreparative RP-HPLC (10 μm C18, Vydac) with elution at 3 mL/min with a linear gradient of 0−90% solvent B over 80 min, using a Waters 600 solvent delivery system (solvent A, 0.1% TFA, solvent B, 90% acetonitrile, 0.09% TFA). Inhibition of activity in an nAChR assay in oocytes (see below) was used to indicate the presence of α-conotoxins in both the SE fractions and in the RP fractions. Additional conopeptides were identified by mass-based selection. The peptides were further purified from both SE and RP-HPLC fractions by RP-HPLC (C18, 5 μm, 46 × 250 mm, Jupiter, with elution at 1 mL/min, or SB300 C18, 3.5 μm, 2.1 × 50 mm, Zorbax, with elution at 0.2 mL/min). Eution was with linear gradients of 0−25% B over 25 or 45 min for AnIB, and 0−70%B over 60 min for more hydrophobic peptides. The components were sequenced after reduction and alkylation with maleimide as described below. Initial mass spectrometry analyses of peptides were conducted with a Micromass LCT mass spectrometer, and by LC/MS analysis as described above.

Sequencing of Native Peptides. The purified peptides (∼20 pmol) were reduced in the presence of 10 mM TCEP and 50 mM ammonium acetate pH 4.5 (37 °C for 1 h) and then alkylated in the added presence of 20 mM maleimide (37 °C for 1 h). The alkylated peptides was repurified by RP-HPLC and submitted for analysis by Edman chemistry using a 492-01 model Procise protein sequencer.

Peptide Synthesis. Seven peptides, variants of the sequence AnIB, were manually assembled by Fmoc-based chemistry, deprotected, and cleaved from resin largely as described previously.[5] The Ramage-type resin used was a Tricyclic Amide Linker (BAChem, 5-Fmoc-amino-10,11-dihydro-5*H*-dibenzo-[*a*,*d*]cycloheptenyl-2-oxyacetyl-DL-Nle-4-benzhydrylamine resin). Cleavage and deprotection of each peptide-resin was with TFA/TIPS/water at 0−4 °C as described previously.[5] Crude reduced peptides were purified as described earlier. The pure, reduced peptides (50 μM) were stirred in aqueous ammonium bicarbonate, 100 mM, pH 7.5−8 for 24−48 h at 24 °C to achieve oxidation. Oxidized peptides were isolated to >95% purity by preparative RP-HPLC (purity was ascertained by analytical RP-HPLC (C18) and LC/MS (C3)), as described above. Verification of identity of the synthetic peptide was undertaken by comparative HPLC analysis of synthetic peptide and native peptide individually and by coinjection of synthetic and native peptides in a 2:1 ratio (peak area) and by MS analyses.

Peptide Quantitation. Peptides were quantified by RP-HPLC using an external reference standard for each peptide. The α-conotoxin standard had been quantified initially by triplicate amino acid analysis.[19]

Electrophysiology. Functional screening of crude venom and functional characterization of AnIB

Expression of nAChRs in *Xenopus* oocytes. RNA preparation, oocyte preparation, expression of rat nAChRs in *Xenopus* oocytes and two-electrode voltage-clamp recording were performed as described previously.[4] Briefly, plasmids containing cDNA encoding rat α3, α4, α7, β2, and β4 nAChR subunits were provided by J. Patrick (Baylor College of Medicine, Houston, TX) and subcloned into the oocyte expression vector pNKS2.[20] cDNAs for the rat α1, β1, γ, and δ subunits of the muscle nAChR were provided by Dr. V. Witzemann (Max-Planck Institute for Medical Research). Oocytes were injected with 50 nL of cRNA (5−50 ng/μL) and kept at 19 °C in ND96 (96 mM NaCl, 2 mM KCl, 1 mM $CaCl_2$, 1 mM $MgCl_2$ and 5 mM HEPES at pH 7.4) supplemented with 50 mg/L of gentamycin (Sigma Chemical Co., St. Louis, MO).

Two-Electrode Voltage-Clamp Recordings. Two-electrode voltage clamp recordings were performed in oocytes 2−10 days after cRNA injection at a holding potential of −70 mV. Pipets were pulled from borosilicate glass (Harvard Apparatus Ltd., Kent, England), filled with 3 M KCl, and had resistances

of <1 MΩ. Membrane currents were recorded using a two-electrode virtual ground circuit on a GeneClamp 500B amplifier (Axon Instruments Inc., Union City, CA), filtered at 200 Hz, and digitized at 1 kHz using a Digidata 1322A interface and v8.2 Clampex software (Axon Instruments Inc.). The perfusion medium was manually switched between ND96 with or without agonist using a Valve Driver II (General Valve Corporation, Fairfield, NJ). ACh (1 μM) (Sigma) was used to activate $\alpha4\beta4$ and $\alpha1\beta1\gamma\delta$ combinations, 100 μM ACh was used to activate $\alpha3\beta2$, $\alpha3\beta4$, and $\alpha4\beta2$ combinations, and 100 μM nicotine (Sigma) was used to activate α7 nAChRs. A fast and reproducible solution exchange (<300 ms) for agonist application was achieved using a 50 μL funnel-shaped oocyte chamber combined with a fast solution flow (~150 μL/s) fed through a custom-made manifold mounted immediately above the oocyte. ACh pulses were applied for 2 s at 4 min intervals. After each application, the cell was superfused for 1 min with agonist-free solution, and the flow was then stopped before agonist solution was reintroduced. Peptide was applied when responses to three consecutive agonist applications differed by less than 10%. After the 1-min agonist washout step was stopped, 5.5 μL of a 10-fold concentrated peptide solution was pipetted directly into the static bath, mixed by repeated pipetting, and incubated for 3 to 10 min prior to addition of agonist. Addition of toxin directly to the recording chamber conserved material and avoided potential adhesion of the toxin to tubing surfaces. Toxin concentrations below 1 nM were also applied by perfusion for 10 to 15 min and resulted in values that were not markedly different. To obtain estimates of potency, concentration−response curves were fitted to the data by the equation % response = $100/\{1 + ([\text{toxin}]/IC_{50})^{n_H}\}$ using Prism software (GraphPad v 3.0 for Macintosh, San Diego, CA). To obtain estimates of toxin washout, agonist responses were measured at 2 min intervals under constant superfusion. For toxin application, oocytes were perfused for 1 min before a 1-min incubation with the toxin followed by the next agonist application. The IC_{50} values were considered significantly different if their 95% Confidence Intervals did not overlap.

Acknowledgment. This research was supported by an ARC Discovery grant (DP0208295). A.N. was supported by a Research Fellowship of the Deutsche Forschungsgemeinschaft (NI 592/2-1). We thank Simon Nevin for screening of crude venom at muscle subtype nAChRs. We acknowledge Chris Wood for Edman sequence analyses of the peptides. We thank David Wilson for assistance with dissection and RP-HPLC fractionations, and Professor Peter Andrews for support during the project.

Abbreviations

ACh, acetylcholine; nAChRs, nicotinic acetylcholine receptors; HPLC, high-performance liquid chromatography; MS, mass spectrometry; LC/MS, liquid chromatography/mass spectrometry; ES-MS, electrospray mass spectrometry; RT, retention time; RP, reversed phase; TFA, trifluoroacetic acid; [Tyr^{16}]AnIB, unsulfated variant of AnIB; AnIB-OH, AnIB variant with free carboxyl C-terminus.

References

(1) McGehee, D. S.; Role, L. W. Physiological diversity of nicotinic acetylcholine receptors expressed by vertebrate neurons. *Annu. Rev. Physiol.* **1995**, *57*, 521−546.
(2) Paterson, D.; Nordberg, A. Neuronal nicotinic receptors in the human brain. *Prog. Neurobiol.* **2000**, *61*, 75−111.
(3) Elgoyhen, A. B.; Vetter, D. E.; Katz, E.; Rothlin, C. V.; Heinemann, S. F.; Boulter, J. α10: A determinant of nicotinic cholinergic receptor function in mammalian vestibular and cochlear mechanosensory hair cells. *Proc. Natl. Acad. Sci. U.S.A.* **2001**, *98*, 3501−3506.
(4) Nicke, A.; Loughnan, M. L.; Millard, E. L.; Alewood, P. F.; Adams, D. J.; Daly, N. L.; Craik, D. J.; Lewis, R. J. Isolation, structure and activity of GID, a novel α4/7-conotoxin with an extended N-terminal sequence. *J. Biol. Chem.* **2003**, *278*, 3137−3144.
(5) Loughnan, M. L.; Bond, T.; Atkins, A.; Cuevas, J.; Adams, D. J.; Broxton, N. M.; Livett, B. G.; Down, J. G.; Jones, A.; Alewood, P. F.; Lewis, R. J. α-Conotoxin EpI, a novel sulfated peptide from *Conus episcopatus* that selectively targets neuronal nicotinic acetylcholine receptors. *J. Biol. Chem.* **1998**, *273*, 15667−15674.
(6) Wolfender, J. L.; Chu, F. X.; Ball, H.; Wolfender, F.; Fainzilber, M.; Baldwin, M. A.; Burlingame, A. L. Identification of tyrosine sulfation in *Conus pennaceus* conotoxins α-PnIA and α-PnIB: Further investigation of labile sulfo- and phosphopeptides by electrospray, matrix-assisted laser desorption/ionization (MALDI) and atmospheric pressure MALDI mass spectrometry. *J. Mass Spectrosc.* **1999**, *34*, 447−454.
(7) Rappsilber, J.; Steen, H.; Mann, M. Labile sulfogroup allows differentiation of sulfotyrosine and phosphotyrosine in peptides. *J. Mass Spectrosc.* **2001**, *6*, 832−833.
(8) Nemeth-Cawley, J. F.; Karnik, S.; Rouse, J. C. Analysis of sulfated peptides using positive electrospray ionization tandem mass spectrometry. *J. Mass Spectrosc.* **2001**, *36*, 1301−1311.
(9) McLachlin, D. T.; Chait, B. T. Analysis of phosphorylated proteins and peptides by mass sepctrometry. *Curr. Opin. Chem. Biol.* **2001**, *5*, 591−602.
(10) Luo, S. Q.; Kulak, J. M.; Cartier, G. E.; Jacobsen, R. B.; Yoshikami, D.; Olivera, B. M.; McIntosh, J. M. α-Conotoxin AuIB selectively blocks alpha 3 beta 4 nicotinic acetylcholine receptors and nicotine-evoked norepinephrine release. *J. Neurosci.* **1998**, *18*, 8571−8579.
(11) Nicke, A.; Samochocki, M.; Loughnan, M. L.; Bansal, P. S.; Maelicke, A.; Lewis, R. J. 2003 α-Conotoxins EpI and AuIB switch subtype selectivity and activity in native versus recombinant acetylcholine receptors. *FEBS Lett.* **2003**, *554*, 219−223.
(12) Huttner, W. B. Protein tyrosine sulfation. *Trends Biochem. Sci.* **1987**, *12*, 361−363
(13) Fainzilber, M.; Hasson, A.; Oren, R.; Burlingame, A. L.; Gordon, D.; Spira, M. E.; Zlotkin, E. New mollusc-specific α-conotoxins block *Aplysia* neuronal acetylcholine-receptors. *Biochemistry* **1994**, *33*, 9523−9529.
(14) Hogg, R. C.; Miranda, L. P.; Craik, D. J.; Lewis, R. J.; Alewood, P. F.; Adams, D. J. Single amino acid substitutions in α-conotoxin PnIA shift selectivity for subtypes of the mammalian neuronal nicotinic acetylcholine receptor. *J. Biol. Chem.* **1999**, *274*, 36559−36564.
(15) Luo, S.; Nguyen, T. A.; Cartier, G. E.; Olivera, B. M.; Yoshikami, D.; McIntosh, J. M. Single-residue alteration in α-conotoxin PnIA switches its nAChR subtype selectivity. *Biochemistry* **1999**, *38*, 14542−14548.
(16) Broxton, N.; Miranda, L.; Gehrmann, J.; Down, J.; Alewood, P.; Livett, B. Leu(10) of α-conotoxin PnIB confers potency for neuronal nicotinic responses in bovine chromaffin cells. *Eur. J. Pharmacol.* **2000**, *390*, 229−236.
(17) Dwoskin, L. P.; Crooks, P. A. Competitive neuronal nicotinic receptor antagonists: A new direction for drug discovery. *J. Pharmacol. Exp. Ther.* **2001**, *298*, 395−402.
(18) McIntosh, J. M.; Santos A. D.; Olivera, B. M. *Conus* peptides targeted to specific nicotinic acetylcholine receptor subtypes. *Annu. Rev. Biochem.* **1999**, *68*, 59−88.
(19) Bidlingmeyer, B. A.; Cohen, S. A.; Tarvin, T. l. Rapid analysis of amino acids using precolumn derivatization. *J. Chromatog.* **1984**, *336*, 93−104.
(20) Gloor, S.; Pongs, O.; Schmalzing, G. A vector for the synthesis of cRNAs encoding Myc epitope-tagged proteins in *Xenopus laevis* oocytes. *Gene* **1995**, *160*, 213−217.
(21) McIntosh, J. M.; Yoshikami, D.; Mahe, E.; Nielsen, D. B.; Rivier, J. E.; Gray, W. R.; Olivera, B. M. A nicotinic acetylcholine-receptor ligand of unique specificity, α-Conotoxin-ImI. *J. Biol. Chem.* **1994**, *269*, 16733−16739.
(22) Zhao, D.; Huang, P. *Conus imperialis* conotoxin ImIIA precursor mRNA. Submitted (NOV-1999) to the EMBL/GenBank/DDBJ databases 1999.
(23) Ellison, M.; McIntosh, J. M.; Olivera, B. M. α-Conotoxins ImI and ImII − Similar α7 nicotinic receptor antagonists act at different sites. *J. Biol. Chem.* **2003**, *278*, 757−764.
(24) Cartier, G. E.; Yoshikami, D. J.; Gray, W. R.; Luo, S. Q.; Olivera, B. M.; McIntosh, J. M. A new α-conotoxin which targets alpha 3 beta 2 nicotinic acetylcholine receptors. *J. Biol. Chem.* **1996**, *271*, 7522−7528.
(25) McIntosh, J. M.; Dowell, C.; Watkins, M.; Garrett, J. E.; Yoshikami, D.; Olivera, B. M. α-Conotoxin GIC from *Conus geographus*, a novel peptide antagonist of nicotinic acetylcholine receptors. *J. Biol. Chem.* **2003**, *277*, 33610−33615.

(26) Martinez, J. S.; Olivera, B. M.; Gray, W. R.; Craig, A. G.; Groebe, D. R.; Abramson, S. N.; Mcintosh, J. M. α-Conotoxin EI, a new nicotinic acetylcholine-receptor antagonist with novel selectivity. *Biochemistry* **1995**, *34*, 14519−14526.
(27) Dowell, C.; Olivera, B. M.; Garrett, J. E.; Staheli, S. T.; Watkins, M.; Kuryatov, A.; Yoshikami, D.; Lindstrom, J. M.; McIntosh, J. M. α-Conotoxin PIA is selective for α6 subunit-containing nicotinic acetylcholine receptors. *J. Neurosci.* **2003**, *23*, 8445−8452.
(28) Sandall, D. W.; Satkunanathan, N.; Keays, D. A.; Polidano, M. A.; Liping, X.; Pham, V.; Down, J. G.; Khalil, Z.; Livett, B. G.; Gayler, K. R. A novel α-conotoxin identified by gene sequencing is active in suppressing the vascular response to selective stimulation of sensory nerves *in vivo*. *Biochemistry* **2003**, *42*, 6904−6911.

JM031010O